coupling provides an effective relaxation mechanism for a coupled ^{13}C nucleus), there is expected to be little difference in $^{59}Co-^{13}C$ coupling in *lel* and *ob* rings. Differences are expected to arise from a dependence of $J(^{59}Co-^{13}C)$ on dihedral angle. The functional relationship for such a dependence should be symmetrical, to a first approximation, about a value of 180° for this angle.[22] Values calculated for Co-N-C-C dihedral angles in *lel* and *ob* rings generated in molecular mechanics calculations[1] are, respectively, +160° and -158° (for *lel,lel,lel*-Δ- and *ob,ob,ob*-Δ-$[Co((\pm)\text{-bn})_3]^{3+}$). The former value is in relatively good agreement with the value of 166.9° observed for the *lel,lel,lel* Co(III) complex.[7] Since the angles expected for *lel* and *ob* rings are spaced nearly equally on either side of 180°, little difference in the coupling constant is expected. On the other hand, it may be that variations in the ^{59}Co quadrupole coupling constant, and hence in $R_1(^{59}Co)$, with geometry differences between isomers, could lead to the observed effect of geometry on methyl group resonance broadening. Studies are now in progress in our laboratory on ^{13}C relaxation in these and related complexes.

(22) Karplus, M. *J. Chem. Phys.* **1959**, *30*, 11.

Acknowledgment. We wish to acknowledge the financial support of the Ministerio de Educación y Ciencia de España for a fellowship provided Dr. Gargallo, the National Science Foundation for an instrument grant for the Syntex $P3/F$ diffractometer and $R3$ structure determination system, and the Research Allocations Committee of The University of New Mexico. We also wish to thank Prof. Hans Toftlund, University of Odense, Denmark, and Prof. Kjeld Rasmussen, The Technical University of Denmark, for their helpful comments and for unpublished data, and Prof. R. Garth Kidd for allowing our use of an unpublished manuscript. Finally we acknowledge the helpful comments of a reviewer who pointed out the possibility that a geometry-induced variation in ^{59}Co quadrupole coupling leads to the observed geometry dependence in methyl group resonance broadening.

Registry No. $[Rh((\pm)\text{-bn})_3]_2(SO_4)_3$, 88667-97-4; $[Co((\pm)\text{-bn})_3]_2(SO_4)_3$, 88589-49-5; $[Rh((\pm)\text{-bn})_3]Br_3$, 88667-98-5; $[Co((\pm)\text{-bn})_3]Br_3$, 88589-50-8.

Supplementary Material Available: A stereoview of *lel,lel,lel*-$[Rh((\pm)\text{-bn})_3]^{3+}$, listings of final anisotropic thermal parameters and observed and calculated structure factors, and a complete table of interatomic distances and angles (9 pages). Ordering information is given on any current masthead page.

Contribution from the Istituto per lo Studio della Stereochimica ed Energetica dei Composti di Coordinazione, CNR, 50132 Florence, Italy

Reductive Intramolecular Hydrogen Transfer in a d^8 Metal Hydride Promoted by CO Addition. An Experimental Study and Its Theoretical Implications

FRANCO CECCONI, CARLO A. GHILARDI, PAOLO INNOCENTI, CARLO MEALLI, STEFANO MIDOLLINI,* and ANNABELLA ORLANDINI

Received May 19, 1983

The nickel(II) hydride $[(np_3)NiH]BPh_4$, np_3 = tris(2-(diphenylphosphino)ethyl)amine, reacts in both the solid state and solution with carbon monoxide, under mild conditions, to yield the nickel(0) carbonyl derivative $[(Hnp_3)NiCO]BPh_4$. The molecular structure of $[(Hnp_3)NiCO]BPh_4 \cdot 0.5C_4H_8O$ has been established by single-crystal X-ray diffraction methods. The crystals are triclinic, space group $P\bar{1}$, with the following cell parameters: a = 18.917 (8), b = 16.341 (7), c = 10.151 (5) Å; α = 94.31 (6), β = 94.27 (6), γ = 96.94 (6)°; Z = 2. The structure has been solved by three-dimensional Patterson and Fourier syntheses and refined by least-squares techniques to final R and R_w factors of 0.073 and 0.073, respectively. The nickel atom is tetrahedrally coordinated by the three phosphorus atoms of the np_3 ligand and by the carbonyl group. A hydrogen atom lies collinear with the nickel and the apical nitrogen atom of the np_3 ligand. The N-H distance, 1.15 (9) Å, indicates a bonding between these two atoms, but the Ni-H distance of 1.95 (9) Å does not exclude some interaction between the hydrogen and the metal atom. The ^1H NMR spectra of $[(Hnp_3)NiCO]BPh_4$ are indicative of N-H bonding, whereas the IR data suggest at least a weak residual Ni-H interaction. Molecular orbital studies of the extended Hückel type indicate that the N-H bond is energetically favored over a possible Ni-H bond and that the Ni-H overlap population drops to zero as the hydrogen approaches the nitrogen atom along the threefold axis of the complex. A Ni-H interaction of electrostatic nature may be predicted from calculated atomic charges. Calculations have been also performed to evaluate a possible migration path of the hydrogen atom from one apical position of the trigonal bipyramid in $[(np_3)NiH]^+$ to the position where is bonded to nitrogen in the carbonyl derivative.

Introduction

Metal hydrides are involved as reagents in the reduction of a wide variety of organic functional groups and as intermediates in numerous catalytic processes. Thus the hydrogen transfer from metal hydrides to organic substrates is a process of general interest.[1]

The results of the reaction of carbon monoxide with hydride complexes can be summarized as follows: (i) CO coordinates to the metal that does not simultaneously affect the metal-hydrogen bond; in this case either the increase in the coordination number or the replacement of the other coligands ensues.[2] (ii) CO coordinates to the metal with cleavage of the metal-hydrogen bond; usually a reductive process occurs with elimination of hydridic hydrogen from the coordination sphere and displacement of H_2 or HX molecules.[3] Sometimes an intramolecular transfer of H^+ to the ligand was observed[4] whereas in a few cases the fate of the hydrogen remained unknown. (iii) CO inserts[5] into the hydrogen-metal bond with

(1) Klinger, R. J.; Mochida, K.; Kochi, J. K. *J. Am. Chem. Soc.* **1979**, *101*, 6626 and references therein.

(2) See, for example: Blake, D. M.; Kubota, M. *J. Am. Chem. Soc.* **1970**, *92*, 2578. Dewhirst, K. C.; Keim, W.; Reilly, C. A. *Inorg. Chem.* **1968**, *7*, 546.

(3) See, for example: Barefield, E. K.; Parshall, G. W.; Tebbe, F. N. *J. Am. Chem. Soc.* **1970**, *92*, 5234. Farmery, K.; Kilner, M. *J. Chem. Soc. A* **1970**, 634. Baird, M. C.; Mague, J. T.; Osborn, J. A.; Wilkinson, G. *Ibid.* **1967**, 1347.

(4) Green, M. L. H.; Wilkinson, G. *J. Chem. Soc.* **1958**, 4314.

0020-1669/84/1323-0922$01.50/0

formation of a formyl derivative. This last reaction has attracted increasing interest, since metal formyl complexes are considered as probable intermediates in the metal-catalyzed reduction of carbon monoxide by molecular hydrogen.[6] Although several experiments have strengthened the suspicion that this reaction, in contrast to alkyl migration, cannot occur to any appreciable extent, two recent papers report the formation of formyl–metal species from the reaction of carbon monoxide with hydride–metal complexes.[7,8] In one case a crystal structure has been reported. In this context it is also worth mentioning a somewhat surprising computational result obtained by Berke and Hoffmann in the course of a theoretical study of organometallic migration reactions.[9] The calculated energy barrier for the hydride shift over a metal-linked CO group is relatively low, actually smaller for the formyl than for the related acetyl formation.

We have now investigated the reaction of CO with the nickel hydride $[(np_3)NiH]BPh_4$ (**1**), where np_3 is the tetradentate tripod ligand tris(2-(diphenylphosphino)ethyl)amine, $N(CH_2CH_2PPh_2)_3$, bearing in mind the following considerations: (a) the closely related methyl complex $[(np_3)NiCH_3]BPh_4$ (**2**) undergoes CO insertion into the nickel–carbon bond under mild conditions;[10] (b) the metal formyl complexes so far isolated appear to be appreciably stable when the –CHO group is linked to a transition-metal center that is coordinatively saturated.[6b,7,11]

We have found that carbon monoxide reacts with **1** to form the pseudotetrahedral derivative $[(Hnp_3)NiCO]^+$ (**3**), $Hnp_3 = HN(CH_2CH_2PPh_2)_3^+$; the fact that the reaction occurs not only in solution but also in the solid state is suggestive of an intramolecular migration of hydrogen over the nitrogen atom of the ligand, with a formal reduction of the metal to the oxidation state 0.

The complexes **1** and **3** were characterized by conductivity measurements and UV, IR, and ^{31}P and ^1H NMR spectra. The crystal structure of **3** has been determined by complete X-ray analysis. Extended Hückel calculations have been performed relating to the problem of the three-center interaction Ni–H–N and to the mechanism of the intramolecular hydrogen migration.

Experimental Section

Unless otherwise stated, all the reactions described were carried out under an atmosphere of dry nitrogen; solvents were purified by standard methods. The ligand np_3[12] and the complex $(np_3)Ni$[13] were prepared by previously described methods. Magnetic, conductometric, and spectrophotometric (both visible and infrared) measurements were carried out with use of methods already described.[14] ^1H and ^{31}P NMR spectra were recorded with a Varian CFT20 spectrometer equipped with ^1H and ^{31}P probes.

Synthesis of the Complexes. $[(np_3)NiH]BPh_4$. Acetic acid (3 mmol) was added, at room temperature, to a solution of $(np_3)Ni$ (2 mmol) in THF (50 mL). The solution quickly turned orange; then sodium tetraphenylborate (2 mmol) in ethanol (20 mL) was added, and the resulting solution was concentrated under a stream of nitrogen. The orange crystals that formed were filtered off and washed with ethanol and then with petroleum ether. Anal. Calcd for $C_{66}H_{63}BNNiP_3$: C, 76.79; H, 6.10; N, 1.35; Ni, 5.69. Found: C, 77.07; H, 6.51; N, 1.29; Ni, 5.51. ^{31}P NMR (C_4D_8O): δ +29.46 s (downfield of H_3PO_4).

$[(Hnp_3)NiCO]BPh_4 \cdot 0.5C_4H_8O$. (A) The solid compound $[(np_3)NiH]BPh_4$ (1 mmol) was placed under carbon monoxide at room temperature and atmospheric pressure. A slow stream of CO was passed through the reaction vessel for the overall time of the experiment. The reaction was monitored by performing IR spectra of the compound. When the ν_{Ni-H} vibration, 1928 cm^{-1}, of the starting compound (**1**) had disappeared (ca. 10 days), the reaction vessel was evacuated and then filled with dry nitrogen. The solid, now cream colored, was dissolved in THF (30 mL), the solution was filtered, and ethanol (20 mL) was added. By concentration under a stream of nitrogen colorless crystals precipitated. They were filtered off and washed with ethanol and then with petroleum ether. Anal. Calcd for $C_{69}H_{66}BNNiO_{1.5}P_3$: C, 75.64; H, 6.07; N, 1.28; Ni, 5.36. Found: C, 75.76; H, 6.34; N, 1.17; Ni, 4.96. ^{31}P NMR (C_4D_8O): δ –1.42 s (upfield of H_3PO_4).

(B) Carbon monoxide was bubbled through a solution of the complex **1** (1 mmol) in tetrahydrofuran (30 mL). The solution rapidly turned pale green, ethanol was added, and the solution was concentrated under a stream of nitrogen until greenish crystals precipitated. They were filtered and washed with ethanol and then with petroleum ether. The compound was recrystallized in air from tetrahydrofuran–*n*-butyl alcohol to give colorless crystals identical with those obtained by method A.

Deuterated Complexes. $[(np_3)NiD]BPh_4$ and $[(Dnp_3)NiCO]BPh_4$ were prepared with the methods used for **1** and **3**, respectively, by using CH_3COOD and C_2H_5OD in the place of CH_3COOH and C_2H_5OH.

Collection and Reduction of X-ray Data. A white parallelepiped-shaped crystal of dimensions 0.80 × 0.18 × 0.05 mm delimited by the faces 100, 010, 001 and the centrosymmetric faces was used for data collection. The sample was mounted on a Philips PW 1100 computer-controlled diffractometer using graphite-monochromated Mo Kα radiation. The temperature during the experiment was 23 ± 2 °C. Cell constants were determined by the least-squares refinement of the setting angles of 24 carefully centered reflections. The crystals are triclinic, space group $P\bar{1}$, with a = 18.917 (8) Å, b = 16.341 (7) Å, c = 10.151 (5) Å, α = 94.31 (6)°, β = 94.27 (6)°, and γ = 96.94 (6)°; the calculated density for two formula units is 1.175 g cm^{-3}. Intensity data were collected within $2\theta < 45°$ at the scan speed of 0.06°/s by using the ω–2θ scan technique with the scan width calculated according to the formula[15] scan range = $A + B \tan \theta$, where A = 0.8° and B = 0.3. Stationary background measurements were taken before and after each scan for a time equal to half the scan time. The intensities of three reflections monitored every 120 min showed variations within ±1%. The intensities were assigned standard deviations calculated as described elsewhere[16] with use of the value of 0.03 for the instability factor k. Of 8058 reflections $(\pm h, \pm k, +l)$, 4102 having $I \geq 3\sigma(I)$ were considered observed. The data were corrected for Lorentz–polarization effects, and an absorption correption giving transmission factors ranging from 0.98 to 0.92 was applied (μ(Mo Kα) = 4.3 cm^{-1}).

Solution and Refinement of the Structure. All the calculations were carried out on a Sel 32/70 computer using the SHELX76 crystallographic system.[17] Atomic scattering factors were taken from ref 18 for the non-hydrogen atoms and from ref 19 for the hydrogen atoms. Both the $\Delta f'$ and $\Delta f''$ components of the anomalous dispersion were included for the non-hydrogen atoms.[20] The function $\sum w(|F_o| - |F_c|)^2$ was minimized during the least-squares refinements, the weights w being defined as $1/\sigma^2(F_o)$.

(5) Although the reaction is more properly termed a migration, here and later in the text we find it convenient to refer to it as an insertion.
(6) (a) Herrmann, W. A. *Angew. Chem., Int. Ed. Engl.* **1982**, *21*, 117. (b) Eisenberg, R.; Hendriksen, D. E. *Adv. Catal.* **1979**, *28*, 79 and references therein.
(7) Wayland, B. B.; Woods, B. A.; Pierce, R. *J. Am. Chem. Soc.* **1982**, *104*, 302. Wayland, B. B.; Woods, B. A. *J. Chem. Soc., Chem. Commun.* **1981**, 700.
(8) Fagan, P. J.; Moloy, K. J.; Marks, T. *J. Am. Chem. Soc.* **1981**, *103*, 6959.
(9) Berke, H.; Hoffmann, R. *J. Am. Chem. Soc.* **1978**, *100*, 7224.
(10) Stoppioni, P.; Dapporto, P.; Sacconi, L. *Inorg. Chem.* **1978**, *17*, 718.
(11) Thorn, D. L.; *Organometallics* **1982**, *1*, 197. Casey, C. P.; Neumann, S. M.; Andrews, M. A.; McAlister, D. R. *Pure Appl. Chem.* **1980**, *52*, 625.
(12) Sacconi, L.; Bertini, I. *J. Am. Chem. Soc.* **1968**, *90*, 5443.
(13) Sacconi, L.; Ghilardi, C. A.; Mealli, C.; Zanobini, F. *Inorg. Chem.* **1975**, *14*, 1380.
(14) Sacconi, L.; Bertini, I.; Mani, F. *Inorg. Chem.* **1968**, *7*, 417.
(15) Alexander, L. E.; Smith, G. S. *Acta Crystallogr.* **1964**, *17*, 1195.
(16) Corfield, P. W. R.; Doedens, R. J.; Ibers, J. A. *Inorg. Chem.* **1967**, *6*, 197.
(17) Sheldrick, G. M. "System of Computing Programs"; University of Cambridge: Cambridge, England, 1976 (adapted by Dr. C. Mealli).
(18) "International Tables for X-ray Crystallography"; Kynoch Press: Birmingham, England, 1974; Vol. IV, p 99.
(19) Stewart, R. F.; Davidson, E. R.; Simpson, W. T. *J. Chem. Phys.* **1965**, *42*, 3175.
(20) "International Tables for X-ray Crystallography"; Kynoch Press: Birmingham, England, 1974; Vol. IV, p 149.

Table I. Positional and Thermal Parameters[a]

atom	x	y	z	U, Å²	atom	x	y	z	U, Å²
Ni	1974 (1)	1714 (1)	3123 (1)	*b*	C(4,5)	73 (4)	2300 (4)	7293 (6)	88 (4)
P(1)	2807 (1)	2220 (2)	1867 (3)	*b*	C(5,5)	644 (4)	1927 (4)	7816 (6)	90 (4)
P(2)	2070 (1)	382 (2)	3284 (3)	*b*	C(6,5)	1281 (4)	1973 (4)	7200 (6)	65 (3)
P(3)	2134 (1)	2419 (2)	5101 (3)	*b*	C(1,6)	2416 (4)	3528 (4)	5126 (6)	45 (3)
N	3469 (4)	1544 (5)	4446 (7)	*b*	C(2,6)	2201 (4)	3935 (4)	4034 (6)	61 (3)
O	588 (4)	1967 (6)	1942 (10)	*b*	C(3,6)	2394 (4)	4786 (4)	4024 (6)	76 (4)
C	1133 (6)	1844 (7)	2424 (11)	*b*	C(4,6)	2803 (4)	5230 (4)	5105 (6)	80 (4)
C(1)	3984 (5)	1844 (6)	3473 (10)	50 (3)	C(5,6)	3018 (4)	4822 (4)	6197 (6)	95 (4)
C(2)	3702 (5)	2538 (6)	2761 (10)	50 (3)	C(6,6)	2825 (4)	3972 (4)	6207 (6)	78 (4)
C(3)	3439 (5)	637 (6)	4619 (9)	46 (3)	C(1,7)	4483 (3)	6776 (4)	2705 (7)	48 (3)
C(4)	2996 (5)	135 (6)	3458 (10)	48 (3)	C(2,7)	4337 (3)	5933 (4)	2860 (7)	71 (4)
C(5)	3537 (5)	2071 (6)	5744 (10)	50 (3)	C(3,7)	4761 (3)	5379 (4)	2308 (7)	78 (4)
C(6)	2805 (5)	2066 (6)	6291 (9)	46 (3)	C(4,7)	5332 (3)	5667 (4)	1602 (7)	78 (4)
C(1,1)	2657 (3)	3132 (5)	1003 (7)	48 (3)	C(5,7)	5479 (3)	6510 (4)	1448 (7)	73 (4)
C(2,1)	3138 (3)	3856 (5)	1108 (7)	66 (3)	C(6,7)	5054 (3)	7065 (4)	1999 (7)	56 (3)
C(3,1)	2986 (3)	4519 (5)	394 (7)	82 (4)	C(1,8)	4095 (4)	7475 (4)	5106 (7)	47 (3)
C(4,1)	2352 (3)	4459 (5)	−424 (7)	85 (4)	C(2,8)	4368 (4)	6839 (4)	5744 (7)	55 (3)
C(5,1)	1871 (3)	3735 (5)	−529 (7)	96 (5)	C(3,8)	4425 (4)	6869 (4)	7126 (7)	67 (3)
C(6,1)	2023 (3)	3071 (5)	184 (7)	75 (4)	C(4,8)	4209 (4)	7533 (4)	7869 (7)	75 (4)
C(1,2)	3001 (3)	1523 (4)	474 (7)	43 (3)	C(5,8)	3936 (4)	8169 (4)	7231 (7)	76 (4)
C(2,2)	2429 (3)	963 (4)	−117 (7)	56 (3)	C(6,8)	3879 (4)	8140 (4)	5850 (7)	60 (3)
C(3,2)	2534 (3)	405 (4)	−1172 (7)	74 (4)	C(1,9)	3113 (4)	7096 (4)	2967 (6)	53 (3)
C(4,2)	3211 (3)	406 (4)	−1635 (7)	73 (4)	C(2,9)	2588 (4)	7214 (4)	3831 (6)	66 (3)
C(5,2)	3782 (3)	966 (4)	−1043 (7)	73 (4)	C(3,9)	1871 (4)	6952 (4)	3421 (6)	86 (4)
C(6,2)	3677 (3)	1524 (4)	11 (7)	57 (3)	C(4,9)	1679 (4)	6571 (4)	2147 (6)	83 (4)
C(1,3)	1683 (3)	−357 (4)	1902 (7)	42 (3)	C(5,9)	2205 (4)	6453 (4)	1283 (6)	88 (4)
C(2,3)	1003 (3)	−259 (4)	1356 (7)	55 (3)	C(6,9)	2922 (4)	6715 (4)	1692 (6)	72 (4)
C(3,3)	663 (3)	−820 (4)	335 (7)	66 (3)	C(110)	4196 (3)	8376 (4)	2861 (6)	44 (3)
C(4,3)	1003 (3)	−1480 (4)	−140 (7)	70 (4)	C(210)	3913 (3)	8526 (4)	1607 (6)	54 (3)
C(5,3)	1683 (3)	−1579 (4)	406 (7)	75 (4)	C(310)	4123 (3)	9274 (4)	1083 (6)	59 (3)
C(6,3)	2023 (3)	−1017 (4)	1427 (7)	65 (3)	C(410)	4616 (3)	9872 (4)	1815 (6)	57 (3)
C(1,4)	1662 (4)	−118 (4)	4649 (7)	48 (3)	C(510)	4900 (3)	9722 (4)	3069 (6)	49 (3)
C(2,4)	1097 (4)	228 (4)	5186 (7)	63 (3)	C(610)	4690 (3)	8974 (4)	3592 (6)	43 (3)
C(3,4)	720 (4)	−172 (4)	6134 (7)	89 (4)	C(1)*	853 (31)	6325 (29)	7170 (62)	253 (13)
C(4,4)	909 (4)	−918 (4)	6545 (7)	90 (4)	C(2)*	262 (33)	6313 (33)	7948 (57)	253 (13)
C(5,4)	1474 (4)	−1264 (4)	6008 (7)	100 (5)	C(3)*	1 (23)	5479 (43)	8082 (55)	253 (13)
C(6,4)	1850 (4)	−864 (4)	5059 (7)	78 (4)	C(4)*	457 (37)	4976 (20)	7452 (62)	253 (13)
C(1,5)	1347 (4)	2393 (4)	6060 (6)	47 (3)	C(5)*	973 (26)	5497 (43)	6862 (55)	253 (13)
C(2,5)	775 (4)	2767 (4)	5537 (6)	79 (4)	B	3978 (6)	7424 (7)	3436 (12)	47 (3)
C(3,5)	139 (4)	2721 (4)	6153 (6)	106 (5)	H	2928 (50)	1578 (53)	3862 (87)	63 (30)

[a] Coordinates are multiplied by 10^4 and temperature factors by 10^3. Carbon atoms marked with an asterisk belong to the solvent molecule and were assigned a population parameter of 0.5. [b] Anisotropic.

The structure was solved by the heavy-atom method. Full-matrix least-squares refinements were carried out by assigning anisotropic thermal parameters to the heavier atoms and by treating the phenyl rings as rigid groups. The hydrogen atoms were introduced in calculated positions but not refined. A difference Fourier map calculated at the *R*-factor value of 0.083 showed several peaks attributable to the tetrahydrofuran molecule and a peak of 0.3 e/Å³ at 1.9 and 1.2 Å from the metal and from the central nitrogen atom of the np_3 ligand, respectively. Since an attempt to refine the solvent molecule gave poor results, this molecule was treated as a rigid group with an overall temperature factor and a population parameter of 0.5. A subsequent difference Fourier map calculated by using the reflections that had $(\sin\theta)/\lambda \leq 0.3$ Å^{-1} confirmed the presence of a peak coaxial with the metal and the nitrogen atoms. This was treated as hydrogen, and its positional and thermal parameters were included in the final least-squares refinement, which converged at the *R* and R_w factors values of 0.073 and 0.073, respectively. The largest shift observed for any of the hydrogen atom parameters in the last cycle was about $^2/_{10}$ of the standard deviations.

The final positional parameters are given in Table I.

Molecular Orbital Calculations. Calculations of the extended Hückel type were carried out with the program ICON8 utilizing the Wolfsberg–Helmholz formula.[21] The atomic parameters for C, O, N, and H species are those standard in the program. The parameters for nickel are as follows: $H_{ii}(3d) = -12.99$ $H_{ii}(4s) = -8.86$, $H_{ii}(4p) = -4.9$; exponents (4s,4p) = 1.9; $\xi_1(3d) = 5.39$, $\xi_2(3d) = 2.0$; contraction coefficients in double-ζ expansion $C_1 = 0.5797$, $C_2 = 0.6182$. The geometrical parameters not specified elsewhere in the text are as follows: Ni–P = 2.25, Ni–C = 2.0, C–O = 1.25, P–H = 1.4, N–H = 1.09 Å; H–P–H = 109.47, H–N–H = 109.47°. The relative orientation of the NH_3 and NiP_3 fragments was taken as staggered.

(21) (a) Hoffmann, R. *J. Chem. Phys.* **1963**, *39*, 1397. (b) Hoffmann, R. Lipscomb, W. N. *Ibid.* **1962**, *36*, 3179, 3489; **1962**, *37*, 2872. (c) Ammeter, I. H.; Bürgi, H.-B.; Thibeault, I. C.; Hoffmann, R. *J. Am. Chem. Soc.* **1978**, *100*, 3686.

Results and Discussion

Synthesis and Properties of the Complexes. As previously reported,[22] the crystals of the nonstoichiometric compounds $[(np_3)NiH_x]Y$ ($0 \leq x \leq 1$, Y = ClO_4, BF_4) contain two vicarious species, namely the diamagnetic trigonal-bipyramidal $[(np_3)NiH]^+$ and the paramagnetic trigonal-pyramidal $[(np_3)Ni]^+$ cations. Samples with the value of *x* practically equal to 1 have been obtained by oxidative addition of HBF_4 (or $HClO_4$) to the nickel(0) complex $(np_3)Ni$.[13] We have now prepared the new derivative $[(np_3)NiH]BPh_4$ (**1**) by reaction of $(np_3)Ni$ with acetic acid and $NaBPh_4$ in THF solution:

$$(np_3)Ni + CH_3COOH + NaBPh_4 \rightarrow [(np_3)NiH]BPh_4 + CH_3COONa$$

The complex **1**, which crystallizes as moderately air-stable orange prisms, is diamagnetic; it is soluble in common polar organic solvents such as acetone, tetrahydrofuran, and 1,2-dichloroethane, in which it behaves as a 1:1 electrolyte. The ^1H NMR spectrum of the compound shows a quadruplet at δ −23.2 (J_{P-H} = 37.5 Hz, CD_3COCD_3, upfield of Me_4Si), due to the hydridic hydrogen atom. The IR spectrum of **1** (see Figure 1) contains a medium-intensity band at 1928 cm^{-1}, which disappears in the spectrum of the deuterated derivative.

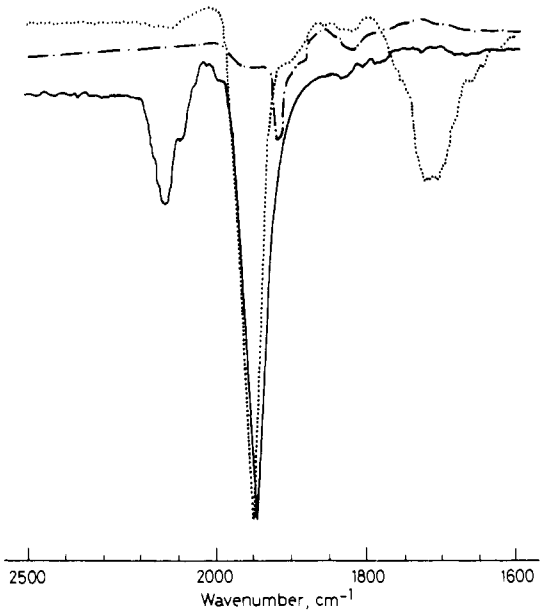

Figure 1. Infrared spectra (Nujol mulls), in the 2500–1600-cm^{-1} region, of the complexes $[(np_3)NiH]BPh_4$ (–·–·), $[(Hnp_3)NiCO]BPh_4 \cdot 0.5THF$ (—), and $[(Dnp_3)NiCO]BPh_4 \cdot 0.5THF$ (···).

Interestingly this band, which must be attributed to the Ni–H stretching vibration, is absent in the spectra of the nonstoichiometric hydrides.[22] On the other hand, the strong IR band at 595 cm^{-1} present in the spectra of the nonstoichiometric hydrides and attributed to a Ni–H vibration is also present in the IR spectrum of **1**. Although the IR spectra differ in some details, nonetheless it seems correct to assume for **1** the same trigonal-bipyramidal structure found for the nonstoichiometric hydride. Moreover, this is the geometry already ascertained by X-ray analysis for the isoelectronic compound $(np_3)CoH$.[13,23]

The solid hydride $[(np_3)NiH]BPh_4$ slowly reacts with CO at room temperature and atmospheric pressure. The crystals decolorize, and the reaction can be monitored by IR spectra: the band at 1928 cm^{-1} progressively disappears while two new bands at 2130 (medium, broad) and 1940 (very strong) cm^{-1} simultaneously appear. The reaction is complete after ca. 10 days to form the colorless compound $[(Hnp_3)NiCO]BPh_4$ (**3**).

When **1** is treated with CO in THF solution, under the same conditions of temperature and pressure, a reaction (ca. 3 min) occurs to give a pale green product. This consists mainly of the colorless compound **3** with some impurities (ca. 1–2%) of the air-unstable green nickel(I) complex $[(np_3)NiCO]BPh_4$[13] (**4**), which confers the specific color on the material. Indeed: (i) The new greenish product has analytical data and ^{31}P and ^1H NMR spectra practically identical with those of **3**. (ii) The IR spectra of the two materials are practically superimposable with the exception of a weak, sharp band at 1990 cm^{-1}, which is present only in the spectrum of the greenish material. This band shows up with an intensity that is variable for different samples obtained from different preparations; moreover, the band is unshifted in the deuterated derivatives and exactly corresponds both in position and in shape to the CO stretching vibration present in the IR spectrum of **4**. (iii) The reflectance spectrum of the greenish material shows the band at ca. 12 130 cm^{-1}, which is present in the corresponding spectrum of **4**. The small amounts of the paramagnetic $[(np_3)NiCO]BPh_4$ are not sufficient to determine a detectable bulk paramagnetism in the greenish material. The pure colorless complex **3**, identical with the compound obtained by reacting CO with the solid compound **1**, can be obtained from crystallization in air of the pale green material.

Table II. Selected Bond Lengths (Å) and Angles (deg)

Ni–P(1)	2.222 (3)	P(2)–C(1,3)	1.828 (7)
Ni–P(2)	2.223 (3)	P(2)–C(1,4)	1.832 (8)
Ni–P(3)	2.220 (3)	P(3)–C(6)	1.859 (9)
Ni–C	1.737 (12)	P(3)–C(1,5)	1.836 (8)
Ni–H	1.95 (9)	P(3)–C(1,6)	1.825 (7)
Ni–N	3.092 (8)	N–C(1)	1.506 (11)
N–H	1.15 (9)	N–C(3)	1.501 (11)
C–O	1.154 (11)	N–C(5)	1.507 (11)
P(1)–C(2)	1.856 (10)	C(1)–C(2)	1.518 (12)
P(1)–C(1,1)	1.826 (8)	C(3)–C(4)	1.518 (12)
P(1)–C(1,2)	1.834 (7)	C(5)–C(6)	1.529 (12)
P(2)–C(4)	1.843 (9)		

P(1)–Ni–P(2)	108.2 (1)	C(4)–P(2)–C(1,3)	101.2 (4)
P(1)–Ni–P(3)	109.0 (1)	C(4)–P(2)–C(1,4)	103.0 (4)
P(2)–Ni–P(3)	111.2 (1)	C(1,3)–P(2)–C(1,4)	99.3 (3)
P(1)–Ni–C	109.9 (4)	Ni–P(3)–C(6)	115.2 (3)
P(2)–Ni–C	110.9 (4)	Ni–P(3)–C(1,5)	116.0 (3)
P(3)–Ni–C	107.6 (4)	Ni–P(3)–C(1,6)	116.4 (2)
P(1)–Ni–H	69 (2)	C(6)–P(3)–C(1,5)	101.8 (4)
P(2)–Ni–H	70 (2)	C(6)–P(3)–C(1,6)	103.5 (4)
P(3)–Ni–H	73 (2)	C(1,5)–P(3)–C(1,6)	101.8 (3)
C–Ni–H	178 (2)	H–N–C(1)	101 (4)
Ni–H–N	171 (6)	H–N–C(3)	102 (4)
Ni–C–O	176.6 (9)	H–N–C(5)	111 (4)
Ni–P(1)–C(2)	114.6 (3)	C(1)–N–C(3)	113.8 (7)
Ni–P(1)–C(1,1)	118.2 (3)	C(1)–N–C(5)	114.3 (7)
Ni–P(1)–C(1,2)	116.2 (2)	C(3)–N–C(5)	113.0 (7)
C(2)–P(1)–C(1,1)	102.4 (4)	N–C(1)–C(2)	109.7 (8)
C(2)–P(1)–C(1,2)	102.9 (4)	C(1)–C(2)–P(1)	112.8 (7)
C(1,1)–P(1)–C(1,2)	100.2 (3)	N–C(3)–C(4)	110.2 (8)
Ni–P(2)–C(4)	114.6 (3)	C(3)–C(4)–P(2)	112.5 (7)
Ni–P(2)–C(1,3)	118.1 (2)	N–C(5)–C(6)	110.0 (8)
Ni–P(2)–C(1,4)	117.9 (2)	C(5)–C(6)–P(3)	112.3 (7)

The complex $[(Hnp_3)NiCO]BPh_4$ is air stable and diamagnetic; the compound is soluble in common polar organic solvents such as tetrahydrofuran, methylene chloride, and nitroethane, in which it behaves as a 1:1 electrolyte. When the complex, in THF solution, is treated with an excess of hydrogen chloride, it does not release a detectable amount of molecular hydrogen.

The complex $[(pp_3)NiH]BPh_4$,[24] pp_3 = tris(2-(diphenylphosphino)ethyl)phosphine, analogously to the methyl derivative $[(pp_3)NiCH_3]BPh_4$,[10] does not seem to be reactive toward carbon monoxide, at room temperature and atmospheric pressure.

Structural Characterization of $[(Hnp_3)NiCO]BPh_4 \cdot 0.5C_4H_8O$. The structure determination of **3** was undertaken to elucidate the fate of the hydridic hydrogen, which in the starting compound $[(np_3)NiH]^+$ (**1**) is reasonably assumed to be coordinated to the metal at one apex of the trigonal bipyramid.

The regular tetrahedral arrangement of four non-hydrogen atoms about the metal, observed in the beginning of the structure solution process, already implied a displacement of hydrogen from the coordination site previously occupied. Moreover, the observed linearity of the M–CO fragment dismissed the possible formation of a formyl group. On account of these points a migration of the hydrogen to the central nitrogen of the np_3 ligand during the reaction from **1** to **3** was supposed. Such a hypothesis was successfully supported by difference Fourier and least-squares techniques. In fact an hydrogen atom between the nitrogen and metal atoms was satisfactorily located and refined. Also, a detailed analysis of the geometrical features of the compound clearly dismisses any doubt that the hydrogen is attached to the amine group of the np_3 ligand.

(22) Sacconi, L.; Orlandini, A.; Midollini, S. *Inorg. Chem.* **1974**, *13*, 2850.
(23) Stoppioni, P.; Dapporto, P. *Cryst. Struct. Commun.* **1979**, *8*, 15.
(24) Cecconi, F.; Midollini, S., unpublished results.

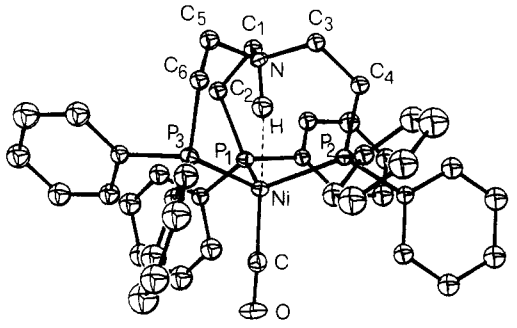

Figure 2. Perspective view of the complex cation $[(Hnp_3)NiCO]^+$ (ORTEP drawing with 30% ellipsoids).

As stated, the metal atom in **3** is tetrahedrally coordinated by three phosphorus atoms of the np_3 ligand and by the carbonyl group. The amine nitrogen atom is located at a nonbonding distance of 3.092 (8) Å from the metal trans to the CO ligand. Figure 2 shows a perspective view of the complex cation, whose selected bond distances and angles are given in Table II. The Ni–C–O grouping is essentially linear with a Ni–C–O angle of 176.6 (9)° and Ni–C and C–O distances of 1.737 (12) and 1.154 (11) Å, respectively. These values compare well with those of 1.74 (2) and 1.18 (2) Å found in the closely related complex $(np_3)NiCO$ (**5**), which has a tetrahedral geometry with the central nitrogen atom at a distance of 3.25 Å from the nickel atom.[25] Such a consistency is also found for the average Ni–P distances 2.222 (1) Å in **3** and 2.215 (5) Å in **5**.

Although in **5** the nitrogen atom is also not coordinated to the nickel atom, there are some differences in **3** that are clearly attributable to the presence of a proton between those two atoms. In **3** there is an enhanced tetrahedral character of the nitrogen atom, the C–N–C angles averaging 113.7 (4)° in **3** vs. 114.7 (3)° in **5**. Although this difference is not very significant, the increased sp^3 character of the nitrogen in **3** clearly shows up from the longer N–C distances (1.505 (2) vs. 1.45 (1) Å). The hydrogen atom also induces some changes in the coordination geometry with the opening of the P–Ni–P angles as compared with those in compound **5** (109.5 (9) vs 106.1 (1)°). These differences are accompanied by a shortening of 0.16 Å of the Ni–N distance in **3** from what is seen in **5**.

Even if the standard deviations are somewhat high, a value of 171 (6)° for the Ni–H–N angle allows the description of the Ni–H–N group as collinear. The Ni–H and N–H distances of 1.95 (9) and 1.15 (9) Å seem to indicate that the proton is mainly bonded to the nitrogen and that a residual Ni–H interaction could be operative. Evidence of this fact comes from the observed Ni–N shortening with respect to the length in the unprotonated compound, **5**, and from a comparison with the structure of the compound $(Et_3NH)[Co(CO)_4]$.[26] Here too a tetrahedral d^{10} metal slightly interacts with the coordinated amine proton. The Co–H interaction, which on the basis of the N–H and Co–H separations, 0.87 (7) and 2.85 (7) Å, respectively, could perhaps be excluded, is on the contrary strongly suggested by the collinearity of the N–H and M–H vectors, as found in our compound. It is indeed remarkable that the ammonium and the metal fragments are here not held together by any collateral bonding network such as the ethylenic chains of the np_3 ligand in **3**; indeed these fragments have been described as ion pairs.[26]

Spectroscopic Characterization of $[(Hnp_3)NiCO]BPh_4$. The IR spectrum of the complex **3** (Nujol mulls) in the region 2500–1600 cm^{-1} is reported in Figure 1 together with that of the corresponding deuterated derivative. The strong band at 1940 cm^{-1} must be obviously assigned to the CO stretching vibration. The broad band at 2130 cm^{-1}, which clearly is due to a vibration involving a hydrogen atom, occurs in the region of the metal–hydride stretching vibrations. However, the fact that the values of the ν_{Ni-H} stretching vibrations are generally observed under 2000 cm^{-1} [27] and mostly the results of the structural analysis seem to be in a better agreement with the assignment of this band to the N–H stretching vibration. The low value of the frequency of this band as compared with those previously reported for ν_{N-H} vibrations in metal complexes containing quaternized ligands[28] may be reasonably expected if one assumes that the N–H bond is weakened by the interaction that the metal exerts on the proton (vide structural analysis). In agreement with such an interpretation the broadness of the band may be consistent with the presence of a M···H–N interaction.

The ^1H NMR spectrum of **3** in CD_2Cl_2 does not show any signal upfield of Me_4Si. This spectrum contains a broad singlet (1 H) at δ 14.55, which is absent in the spectrum of the deuterated derivative. This signal can be likely attributed to the unique nitrogen-bonded hydrogen. A band at δ 9.1 (C_6D_6) has been reported for the N–H hydrogen in the adduct $(Et_3NH)[Co(CO)_4]$.[26]

Molecular Orbital Studies. All the previous chemical, spectroscopic, and crystallographic results, besides the very general question concerning the reasons for the unaccomplished formation of the formyl fragment, raise other questions of more specific interest. We have focused our attention on the following subjects: (i) a description in terms of molecular orbital theory of the three-center interaction Ni–H–N, which seems interesting also for the implications for the chemistry of the ion pairs;[29] (ii) the determination of a possible reaction path that, upon attack of CO on the complex $[(np_3)NiH]^+$, allows the migration of hydrogen to the nitrogen atom. The method used was extended Hückel.

Figure 3a shows the total energy variation for moving the H atom along the straight line Ni–H in the model $[(NH_3)H(PH_3)_3NiCO]^+$ (I) with C_{3v} symmetry. All the C–Ni–P and

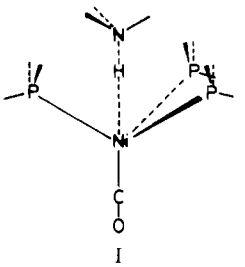

I

P–Ni–P angles were assigned the ideal tetrahedral value, and the Ni–N distance was fixed at 3.0 Å. The computational method (EHMO) works at best poorly in optimizing bond distances; however, the diagram shows that the greatest stabilization occurs for long Ni–H distances. Figure 3b shows the evolution of some important MO levels. The e(*xy*,*yz*) and $2a_1$ orbitals are substantially metal centered, and since the amine is far from the metal, they can be associated with the t_2 set of a tetrahedral complex. The level $1a_1$ is essentially the amine lone pair. An intermediate e level is not shown in Figure 3b. The presence of H affects the orbitals of a_1 symmetry. How the orbitals interact is shown in II. At short

(25) Ghilardi, C. A.; Sabatini, A.; Sacconi, L. *Inorg. Chem.* **1976**, *15*, 2763.
(26) Calderazzo, F.; Facchinetti, G.; Marchetti, F.; Zanazzi, P. F. *J. Chem. Soc., Chem. Commun.* **1981**, 181.
(27) Jesson, J. P. "The Hydrogen Series"; Marcel Dekker: New York, 1971; Vol. 1, p 102.
(28) Di Vaira, M.; Midollini, S.; Sacconi, L. *Inorg. Chem.* **1978**, *17*, 816. Quagliano, J. V.; Banerjee, A. K.; Gaedken, V. L.; Vallarino, L. M. *J. Am. Chem. Soc.* **1970**, *92*, 482.
(29) Swarcz, M., Ed. "Ions and Ion Pairs in Organic Reactions"; Wiley: New York, 1972 (Vol. *1*), 1974 (Vol. 2). Collman, J. P.; Cawse, J. N.; Brauman, J. I. *J. Am. Chem. Soc.* **1972**, *94*, 5905.

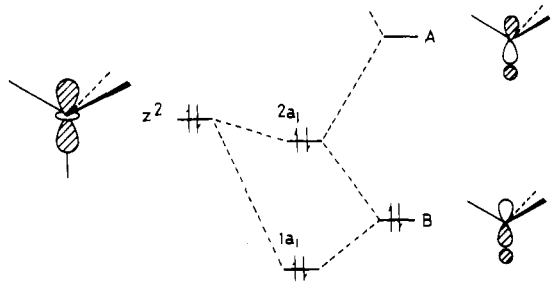

II

N–H distances (Ni–H = ca. 2.0 Å) there is a large splitting between the bonding (B) and antibonding (A) orbitals since they are combinations of the H_s and N_{p_z} orbitals, which are of comparable energy. The lengthening of N–H reduces not only the A–B but also the z^2–A and z^2–B gaps. Thus the $2a_1$ level, predominantly metallic in the beginning, receives progressively larger contributions from both A and B. III shows

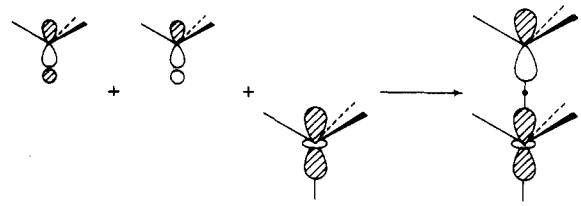

III

how the H_s orbital almost vanishes in the formation of $2a_1$, which then assumes a typical M–N antibonding character. On removal of H from N, A drops and B rises in energy at a speed that is actually larger for A. This involves the latter combination more and more in the formation of $2a_1$ with a net stabilizing effect on its energy. However, only at short Ni–N distances does this stabilization prevail over the destabilization of $1a_1$, which comes from the loss of N–H bonding. At a point close to the crossover between the $2a_1$ and e levels the energy is highest. It is noteworthy that on the side of short Ni–H distances, which still are physically significant, the total energy is higher than on the other side of the barrier. Thus the EH method predicts a structure with a N–H bond but does not say very much about the residual Ni–H bonding that was clearly indicated by previous considerations (see the preceeding sections of the paper). In fact for long Ni–H distances the corresponding overlap population drops to values very close to zero, although still positive; this is mainly a consequence of the fact that the H_s orbital almost cancels in $2a_1$. On the other hand, the electron density donated from nitrogen does not quench the positive charge of the proton, which thus "feels" the negative charge of the tetrahedrally cordinated d^{10} metal atom. Indirectly the EH method warns about the importance of the electrostatic forces which are not included in the calculations.

We now turn to the possible mechanism of CO attack on the hydride complex **1** and to the migration path that leads the H atom to "tunnel" to the same side as the nitrogen atom. Most important for the reaction to occur is the flexibility of the d^{10}–(np_3) fragment, which can easily interconvert as shown in IV. Figure 4 shows the total energy variation (part a) for

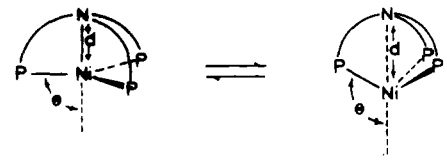

IV

the process and the evolution of some important orbitals (part b). The geometrical deformation is monitored through a

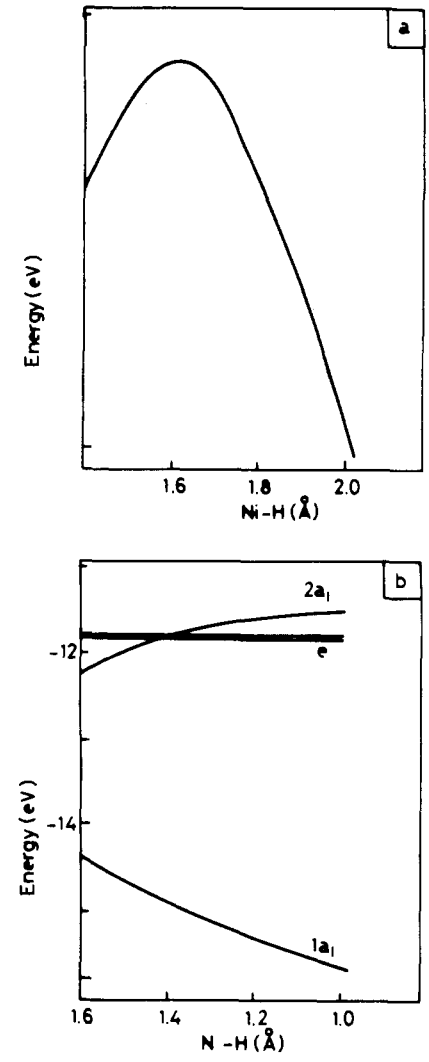

Figure 3. (a) Total energy variation for moving the hydrogen atom along the threefold axis of the $[(NH_3)H(PH_3)_3NiCO]^+$ model (I). (b) Evolution of some important orbitals.

combined variation of θ and d parameters.[30] A small barrier (ca. 7–8 kcal/mol) is calculated and a minimum is also found at a M–N distance of ca. 2.9 Å (θ = ca. 110°). The $1a_1$ level consists mainly of the amine lone pair in a bonding combination with the metal z^2 orbital. The rupture of the M–N bond clearly raises the energy of this level. The orbital $2a_1$ is the corresponding antibonding combination. Elian and Hoffmann,[31] in analyzing the C_{3v} deformation of $(CO)_4M$ fragments, showed that the equivalent of $2a_1$ is destabilized as θ is increased;[32] however, at variance with our deformation path, they kept the parameter d fixed at bonding values. Now we find that the effect of simultaneously removing the apical ligand is stabilizing for $2a_1$. In the initial stages of the deformation the release of M–N antibonding in $2a_1$ is not such as to compensate other increasing destabilizing effects[31] on $1a_1$, 2e, and $2a_1$ levels, hence the origin of the barrier. If a PH_3 molecule is substituted for NH_3, in the attempt to create a suitable model for the polydentate ligand tris(2-(diphenylphosphino)ethyl)phosphine, pp_3, a large energy barrier (ca. 40 kcal/mol) is calculated. In fact the large diffuseness of

(30) A linear relationship between these two parameters was experimentally determined from a number of structures containing the variously elongated np_3 ligand. For previous application and references see: Mealli, C.; Sacconi, L. *Inorg. Chem.* **1982**, *21*, 2870.
(31) Elian, H.; Hoffmann, R. *Inorg. Chem.* **1975**, *14*, 1058.
(32) Notice that in the Elian and Hoffmann paper θ corresponds to the supplementary angle defined by us.

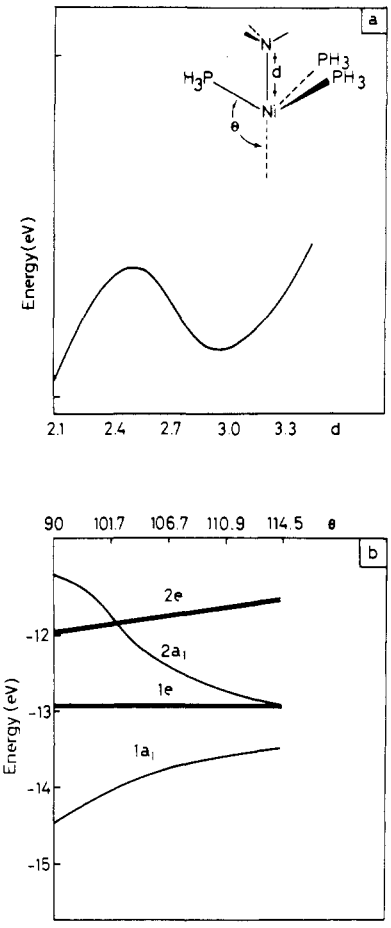

Figure 4. (a) Total energy variation for the interconversion process of the $(NH_3)(PH_3)_3Ni$ model (IV). (b) Evolution of the frontier orbitals for the same process.

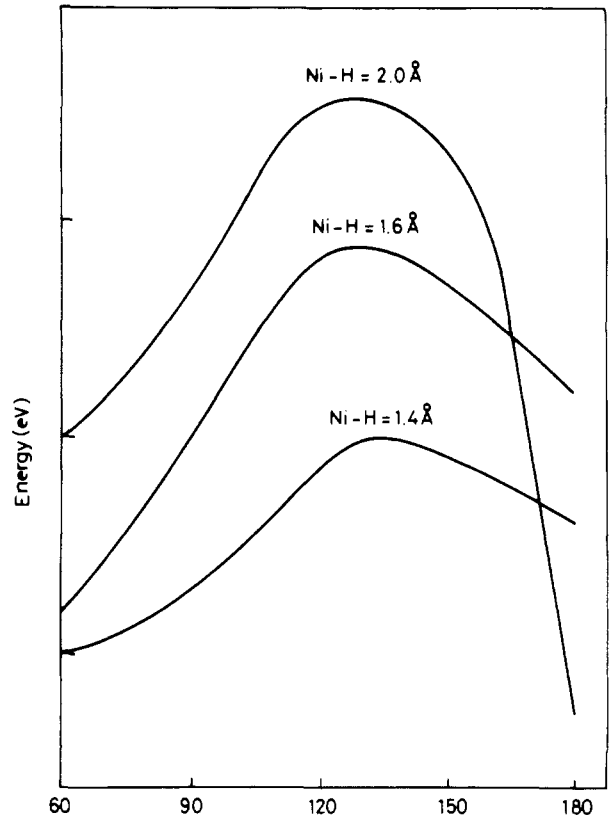

Figure 5. Total energy variation as a function of the angle defined in VII. The three curves refer to different Ni–H separations. The Ni–H distance of 2.0 Å corresponds to a N–H distance of 1.0 Å at $\phi = 180°$; this is also the model that best describes the structure of complex **1** and has the lowest energy.

the phosphine σ lone pair does not allow a sizable reduction of the $M-P_{ap}$ σ antibonding at least in the range 2.1–2.6 Å of $M-P_{ap}$ distances. These arguments account for an experimental fact well-known in this laboratory: all of the complexes that are formed through an elongation of the np_3[33] ligand do not form with the pp_3 analogue.[34]

We have intentionally focused the attention on the deformation capabilities of the metal–polydentate ligand fragment because only through a removal of the apical nitrogen atom does the $[(np_3)NiH]^+$ complex open a new coordination site to carbonyl. The mechanism, already proposed for the insertion of CO into the complex $[(np_3)NiCH_3]^+$,[10] is supported by the present calculations. When, as shown in V, the elongation of the $(NH_3)(PH_3)_3Ni$ fragment is accompanied by the rotation ϕ of the Ni–H vector in the xz plane, besides the expected minimum at the trigonal-bipyramidal geometry (ground state), a second minimum is found in the energy surface at $\phi = 60°$ and $d \simeq 3.0$ Å ($\theta \simeq 111°$). This structure is indeed more destabilized by ca. 20 kcal/mol but has a free coordination site for the carbonyl to enter. A model having CO linked to the metal (Ni–C = 2.0 Å, H–Ni–C = 80°) of the $(NH_3)(PH_3)_3NiH^+$ fragment, which is structured as at the second energy minimum, is already somewhat more stabilized than the two separated fragments which ground-state geometry. The elongated $(NH_3)(PH_3)_3Ni$ fragment, where the amine is practically removed from the coordination sphere, can be thought of as a classical hemioctahedral d^{10} ML_3 fragment[35] that has two filled S and A hybrids and one empty high-lying metal sp hybrid, all shown in VI. In the model

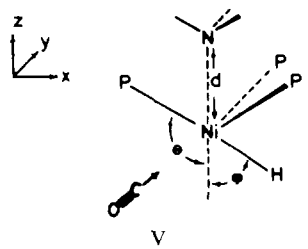

V

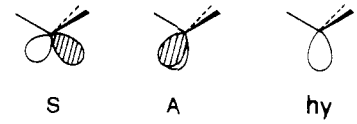

VI

above, S is best directed to overlap with H_s, whereas A is suited for π-back-bonding interaction with a CO π^* orbital. Readjusting the geometry as to bring CO collinear with the ML_3 threefold axis (VII) costs little energy. In fact some loss of π back-donation is compensated by an improved σ donation from CO into the empty metal sp hybrid. Indeed VII is the typical almost tetrahedral coordination of isoelectronic transition-metal hydrides such as $HCo(PF_3)_4$[36] and $HRh(PPh_3)_4$.[37] These complexes, rather than being trigonal bipyramids, are

(33) Some classical examples can be found in ref 13 and in: Mealli, C.; Midollini, S.; Sacconi, L. *Inorg. Chem.* **1978**, *17*, 632. Cecconi, F.; Dapporto, P.; Midollini, S.; Sacconi, L. *Ibid.* **1978**, *17*, 3292. Di Vaira, M.; Ghilardi, C. A.; Sacconi, L. *Ibid.* **1976**, *15*, 1555. Dapporto, P.; Midollini, S.; Sacconi, L. *Angew. Chem., Int. Ed. Engl.* **1979**, *91*, 510.
(34) Unpublished results from this institute.
(35) Albright, T. A. *Tetrahedron* **1982**, *38*, 1339.
(36) Frenz, B. A.; Ibers, J. A. *Inorg. Chem.* **1970**, *9*, 2403.
(37) Baker, R. W.; Pauling, P. *J. Chem. Soc., Chem. Commun.* **1969**, 1495.

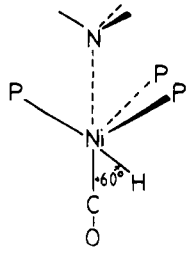

VII

tetrahedrons with the H atom buried in the cavity of three *fac* ligands. Nonetheless, in our case the hydrogen atom chooses to migrate to another cavity of the tetrahedron, the one capped by the nitrogen atom. It could have migrated to the carbon atom to yield a formyl fragment but evidently prefers a tunneling through the coordination plane P–Ni–P to eventually bind to the amine nitrogen atom. We have computationally followed this migration path by varying the ϕ angle defined in VII in the range 60–180°. An energy barrier is calculated at $\phi = 125°$ corresponding to the crossing of the P–Ni–P plane where the hydrogen feels the greatest repulsion of the phosphorus atoms. As shown in Figure 5, the height of the barrier increases from ca. 20 to ca. 60 kcal/mol as the Ni–H distance increases from 1.4 to 2.0 Å on account of the progressively shorter P–H contacts; it can then be reasonably assumed that an opening of the P–Ni–P angle, if allowed by the chained tripodal ligand, can work to reduce the barrier. Also notice that at $\phi = 60°$ the bonding interaction between the H_s orbital and the metal hybrid (VIII) is significantly stronger than that

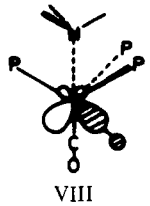

VIII

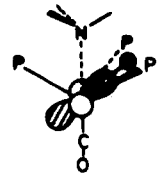

IX

at $\phi = 125°$, shown in IX, where the metal orbital is unhybridized. It is thus probable that the elongation of the metal–hydrogen distance occurs in the final stages of the migration only after the crossing of the coordination plane. Recently Silvestre and Albright[38] have described the motion of an electrophilic atom around a d^{10} tetrahedral complex. They found a soft energy surface, but at variance with our model, a quite long distance between the metal and the electrophilic atom (2.7 Å) was used; in this manner also the difference between the interactions shown in VIII and IX is softened.

(38) Silvestre, I.; Albright, T. A., submitted for publication.

We have dismissed this possibility in our case because it seems unlikely that the H atom after having gone so far from the metal then falls back in between the metal and the nitrogen atom.

The attack of carbonyl on the hydride complex **1** and the consequent migration of H as a proton to the amine group corresponds in practice to a reduction of the metal. The calculated charge of hydrogen, when it occupies one apex of the trigonal-bipyramidal model of compound **1**, is fairly negative but is already slightly positive in model VII, a result in agreement with the suggestion[21] that the more tetrahedral the L_4M fragment, the less hydridic the hydrogen in the adduct $[L_4MH]^+$. The amount of electron density donated from the metal varies along the migration pathway. In VIII the donation is larger than in IX and in between the hydrogen is most positive. When H is trans to CO, its charge would be approximately equivalent to that in VIII if the amine were absent; since the amine captures the proton, the metal remains highly negative, its charge being calculated almost 3 times larger than that in VIII. The formal transformation of the metal from d^8 to d^{10} is completed.

A decrease of the ϕ angle from 60° (see VII) corresponds to the initial stage of the pathway that eventually leads to the formyl fragment. In this paper we will not present a detailed description of the pathway that has indeed many similarities to that described by Berke and Hoffmann for the organometallic migration in $(CO)_5MnR$ (R = H, CH_3) models.[9] We also calculate that a migration to CO costs less energy for H than for CH_3. We point out here a possible cause of the failure of the extended Hückel method in correctly predicting the reactivity in these compounds. As mentioned above, the hydrogen atom is already slightly positive at $\phi \simeq 60°$ when it overlaps with the metal orbital that has the largest donor capability (see VIII). Either an increase or a decrease of ϕ induces a larger positive charge on hydrogen. There may be a sizable electrostatic repulsion with the carbon atom of CO, which is an electrophilic center itself. As is well-known, the EHMO method is not sensitive to these effects. However, a migrating CH_3 group contains some electron density of its own and it is unlikely that it becomes a totally acceptor CH_3^+ group, hence the origin of its more facile nucleophilic attack on carbonyl.[10] Under these circumstances we think that only an ab initio calculation can provide an adequate rationalization of the different behavior of H and CH_3 toward migration to a coordinated CO molecule.

Registry No. **1**, 88510-48-9; **3**·0.5C_4H_8O, 88510-49-0; **4**, 54516-85-7; $(np_3)Ni$, 52633-73-5; deuterium, 7782-39-0.

Supplementary Material Available: Listings of the anisotropic thermal parameters, the calculated hydrogen atom positions, and the structure factor amplitudes (25 pages). Ordering information is given on any current masthead page.